Modes

in Classical and Quantum Optics

Claude Fabre

Covariance Matrix

single mode case :

$$\begin{bmatrix} \Delta^2 E_{X1} & C(E_{X1}E_{Y1}) \\ C(E_{Y1}E_{X1}) & \Delta^2 E_{Y1} \end{bmatrix}$$

two-mode case:

$$\left[\begin{array}{cc|cc} \Delta^2 E_{X1} & C(E_{X1}E_{X2}) & C(E_{X1}E_{Y1}) & C(E_{X1}E_{Y2}) \\ C(E_{X2}E_{X1}) & \Delta^2 E_{X2} & C(E_{X2}E_{Y1}) & C(E_{X2}E_{Y2}) \\ \hline C(E_{Y1}E_{X1}) & C(E_{Y1}E_{X2}) & \Delta^2 E_{Y1} & C(E_{Y1}E_{Y2}) \\ C(E_{Y2}E_{X1}) & C(E_{Y2}E_{X2}) & C(E_{Y2}E_{Y1}) & \Delta^2 E_{Y2} \end{array}\right]$$

symmetric, positive matrix, therefore diagonalizable

"principal component analysis"

Recherche de modes propres: cas mono-quadrature et N modes

$$\begin{bmatrix} \Delta^2 E_{X1} & C(E_{X1}E_{X2}) & \dots & C(E_{X1}E_{XN}) \\ C(E_{X2}E_{X1}) & \Delta^2 E_{X2} & \dots & C(E_{X2}E_{XN}) \\ \dots & \dots & \dots & \dots \\ C(E_{XN}E_{X1}) & C(E_{XN}E_{X2}) & \dots & \Delta^2 E_{XN} \end{bmatrix}$$

généralisable à N modes: N modes propres existent

$$\begin{bmatrix} \Delta^2 E_{X'1} & 0 & 0 & 0 \\ 0 & \Delta^2 E_{X'2} & 0 & 0 \\ \dots & \dots & \dots & \dots \\ 0 & 0 & 0 & \Delta^2 E_{X'N} \end{bmatrix}$$

Selected for a Viewpoint in *Physics*

PRL **104,** 100601 (2010) PHYSICAL REVIEW LETTERS week ending 12 MARCH 2010

Measuring the Transmission Matrix in Optics: An Approach to the Study and Control of Light Propagation in Disordered Media

S. M. Popoff, G. Lerosey, R. Carminati, M. Fink, A. C. Boccara, and S. Gigan

Institut Langevin, ESPCI ParisTech, CNRS UMR 7587, ESPCI, 10 rue Vauquelin, 75005 Paris, France

(Received 27 October 2009; revised manuscript received 11 January 2010; published 8 March 2010)

We introduce a method to experimentally measure the monochromatic transmission matrix of a complex medium in optics. This method is based on a spatial phase modulator together with a full-field interferometric measurement on a camera. We determine the transmission matrix of a thick random scattering sample. We show that this matrix exhibits statistical properties in good agreement with random matrix theory and allows light focusing and imaging through the random medium. This method might give important insight into the mesoscopic properties of a complex medium.

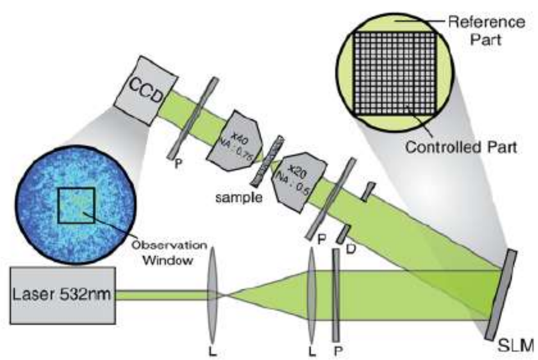

FIG. 1 (color online). Schematic of the apparatus. The laser is expanded and reflected off a SLM. The phase-modulated beam is focused on the multiple-scattering sample and the output intensity speckle pattern is imaged by a CCD camera: lens (L), polarizer (P), diaphragm (D).

Transmission through scattering medium

Monochromatic speckle

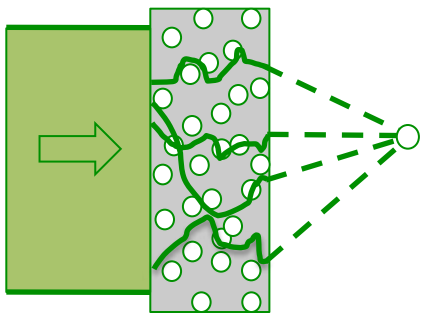

A speckle grain =

- Sum of different paths with random phases
  = *random walk in the complex plane*
- Size limited by diffraction
- Intensity distribution $P(I) \propto \exp^{-I/\langle I \rangle}$
- unpolarized speckle = 2 independent speckles

Polychromatic (i.e. temporal)

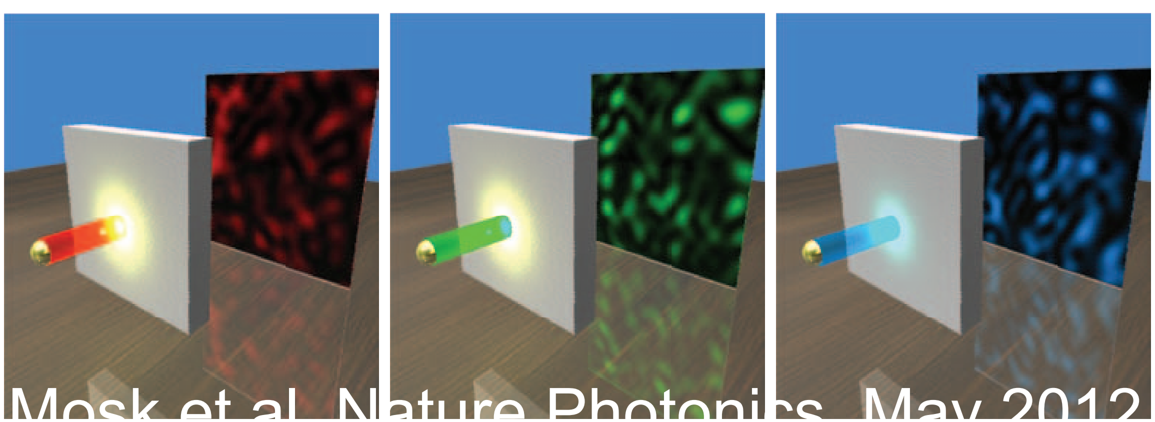

Spectral dependence/ confinement time of light in the medium

Speckle figure : complex distribution … but **coherent** and **deterministic**

Device for wavefront control

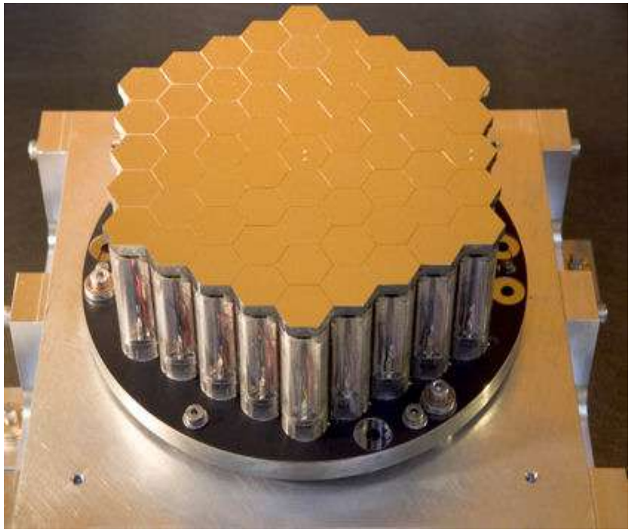

Deformable mirrors
(piezo, magnetics…)

10-100 actuators (typ.)
course : 10-20 microns
Speed > kHz

Adaptive optics

Spatial light modulator (SLM)
(mostly liquid crystals)

Segmented, >1 million pixel
course : 1 microns
speed: <50Hz

Diffractive optics, displays ….

Transmission matrix measurement and use

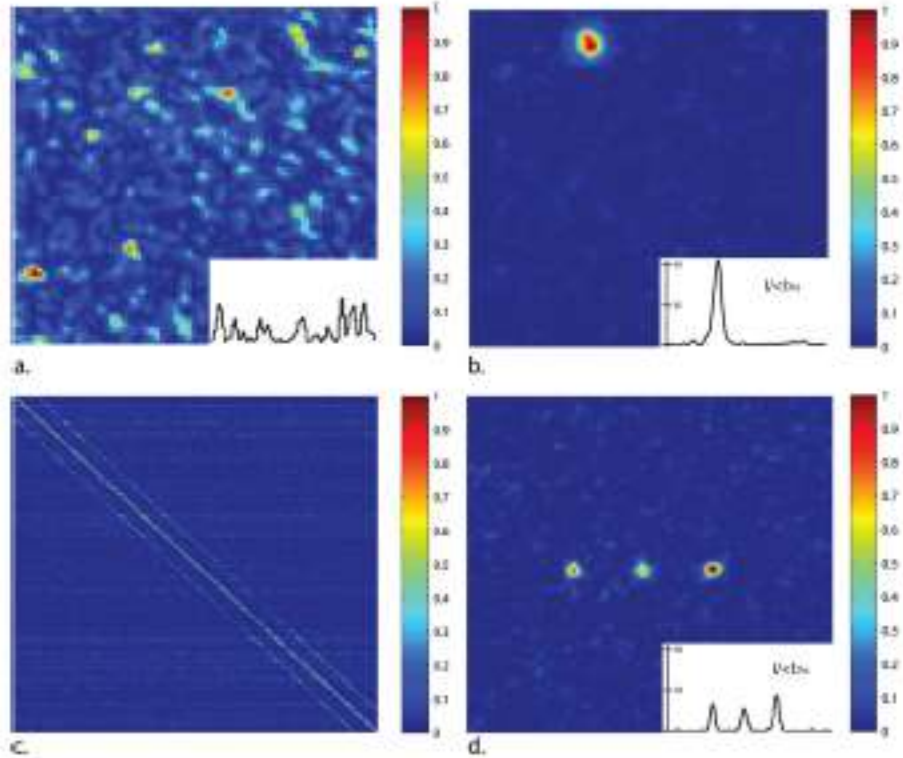

FIG. 2 (color online). Experimental results of focusing. (a) Initial aspect of the output speckle. (b) We measure the TM for 256 controlled segments and use it to perform phase conjugation. (c) Norm of the focusing operator $O^{\mathrm{foc}}_{\mathrm{norm}}$. (d) Example of focusing on several points. (The insets show intensity profiles along one direction.)

singular value decomposition of the transmission matrix
valid for any matrix

$$M=U.\mathrm{diag}(\lambda).V \qquad \text{U, V unitaries}$$

histogram
of singular values

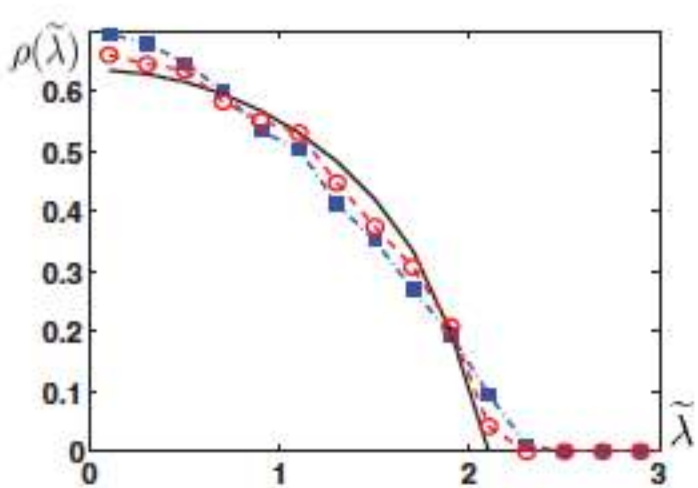

FIG. 4 (color online). Singular value distribution of the experimental transmission matrices obtained by averaging over 16 realizations of disorder. The solid line is the quarter-circle law predicted for random matrices. With the solid squares the matrix filtered to remove the reference amplitude contribution and with the circles the matrix obtained by filtering and removing neighboring elements to eliminate interelement correlations.

Spatial multiplexing in Telecommunications

MIMO capacities and outage probabilities in spatially multiplexed optical transport systems

Peter J. Winzer* and Gerard J. Foschini
Bell Labs, Alcatel-Lucent, 791 Holmdel-Keyport Rd., Holmdel, New Jersey 07733, USA
**peter.winzer@alcatel-lucent.com*

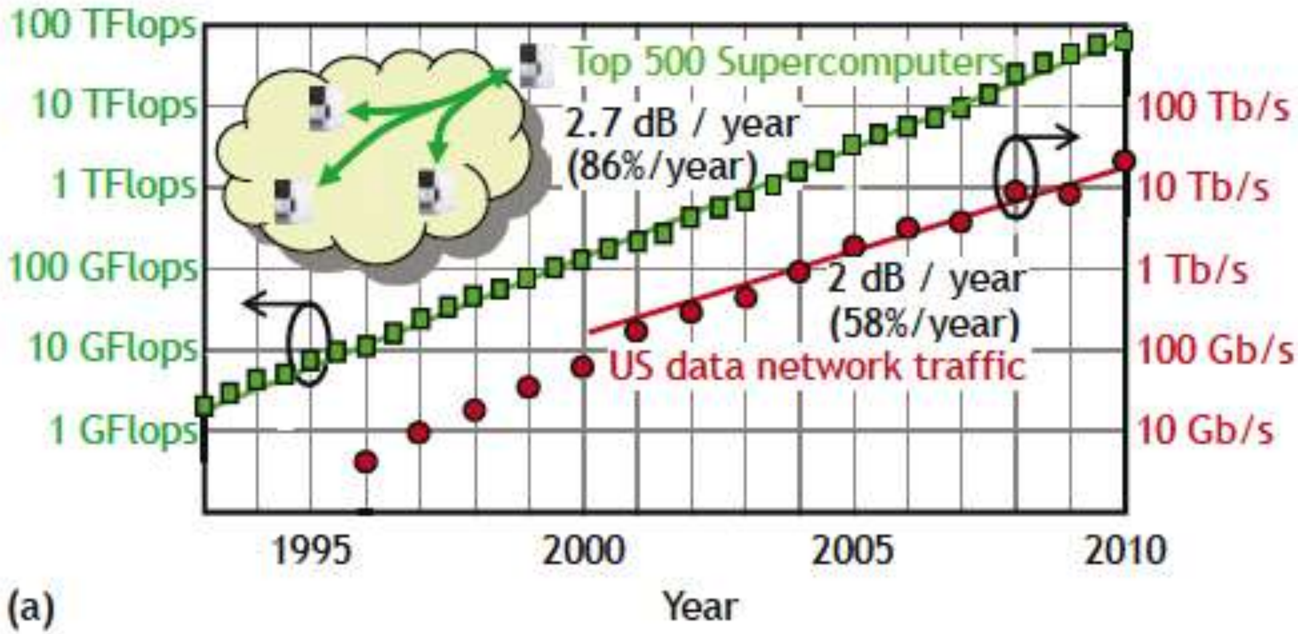

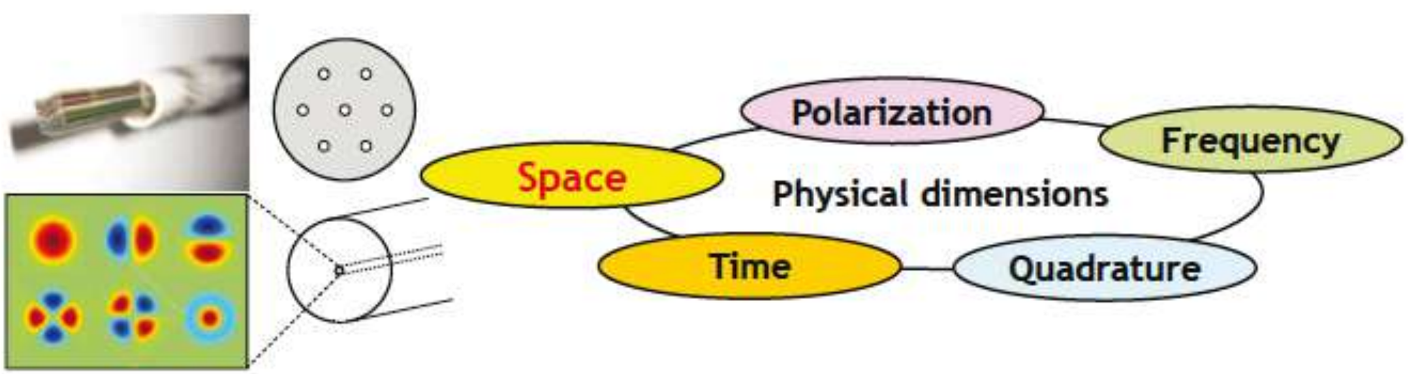

Fig. 2. Spatial multiplexing exploits the only known physical dimension that has not yet been used in optical transport systems. Implementations include fiber bundles, multi-core, and multi-mode fiber (Fig. after [10]).

The MIMO concept

Multiple (modes) In Multiple (modes) out

find the eigenstates of propagation

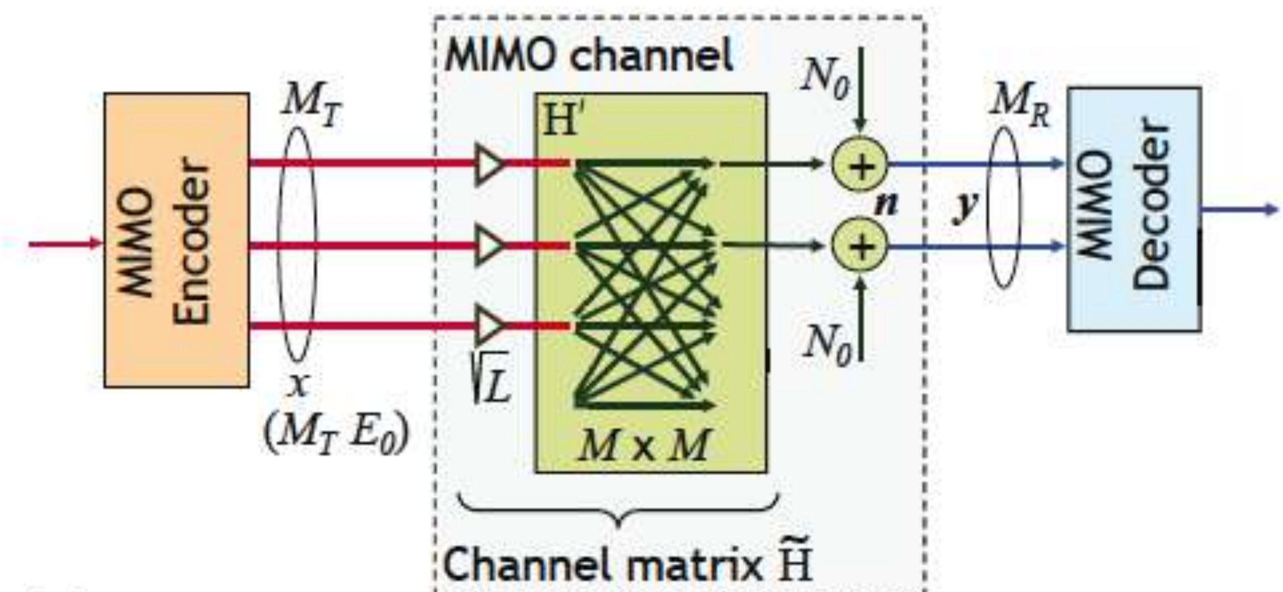

(a)

Coherent Optical MIMO (COMIMO)

Akhil R. Shah, Rick C. J. Hsu, Alireza Tarighat, *Student Member, IEEE*, Ali H. Sayed, *Fellow, IEEE*, and Bahram Jalali, *Fellow, IEEE*

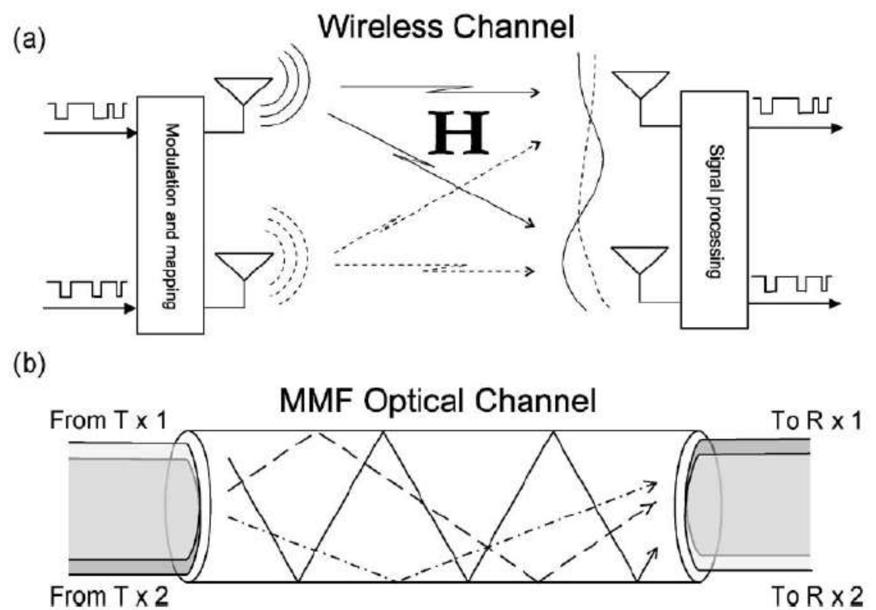

Fig. 1. (a) Coupling diversity into and out of MMF. (b) Ray tracing conceptual description of light beam scattering inside a multimode fiber.

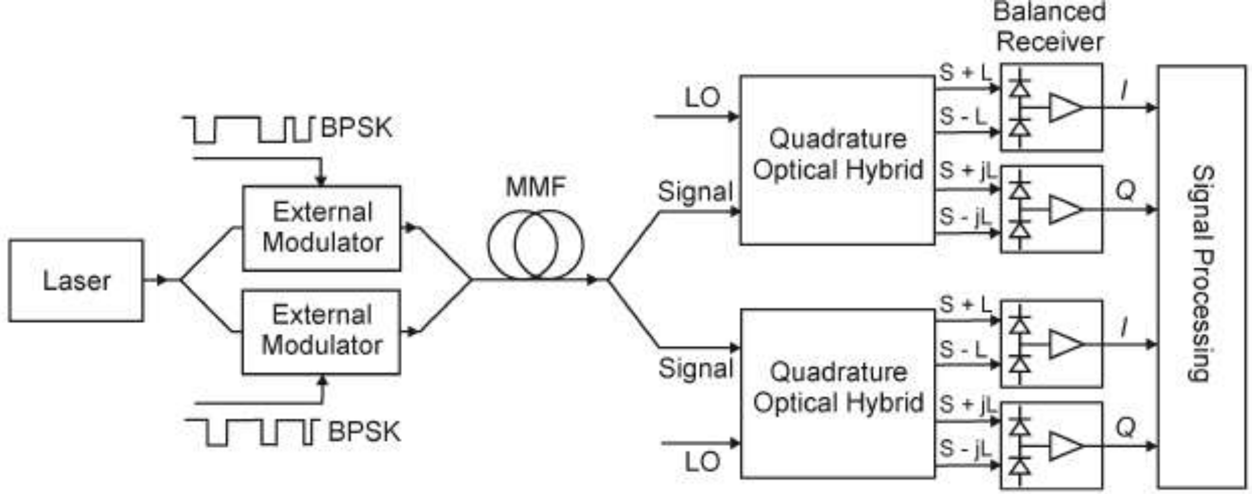

Fig. 2. Block diagram of COMIMO showing two independently modulated carriers and two receivers. Coupling diversity is not shown for simplicity.

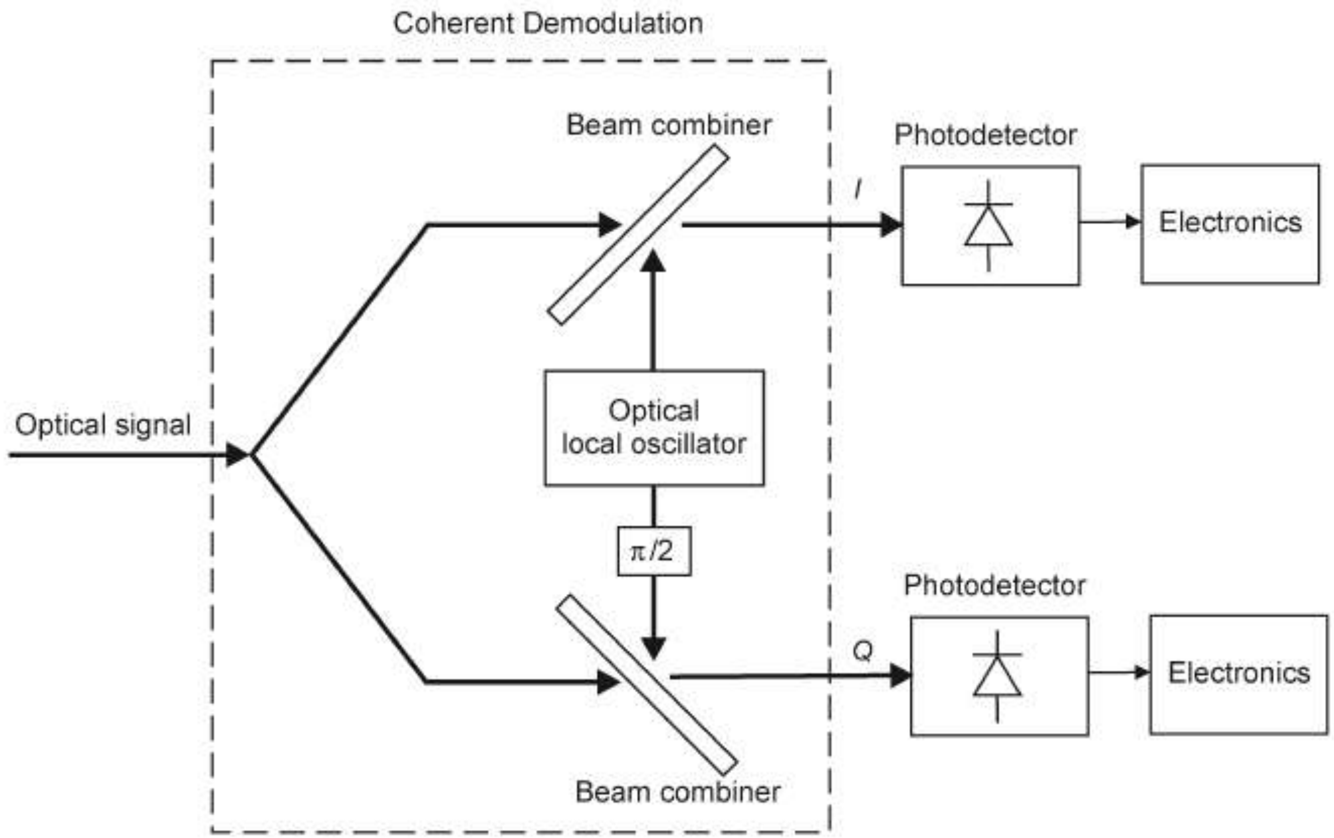

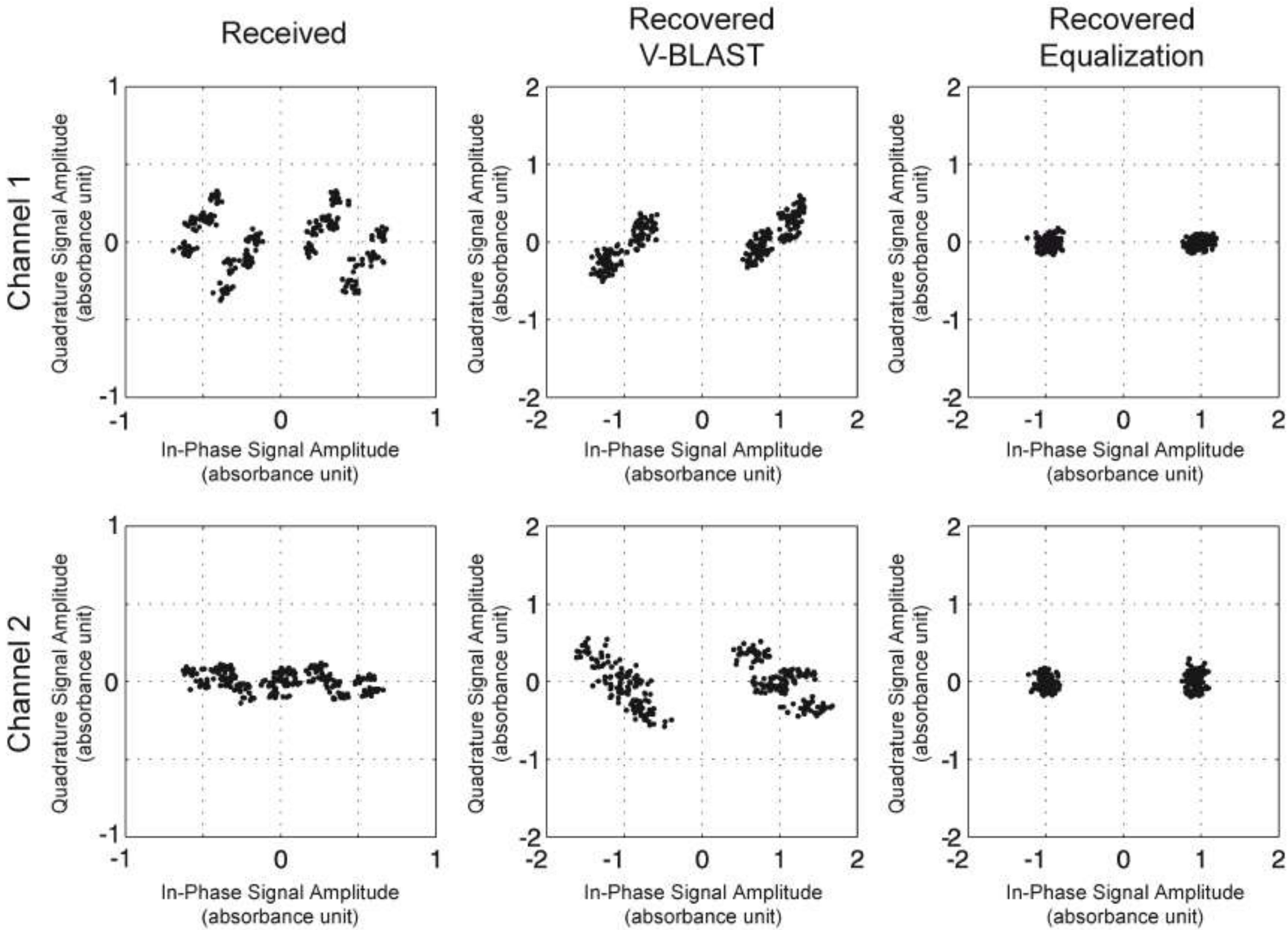

Fig. 5. Constellation diagrams showing received data from a wide-band channel (with ISI) and symbol recovery without equalization and with equalization.

FIELD QUANTIZATION

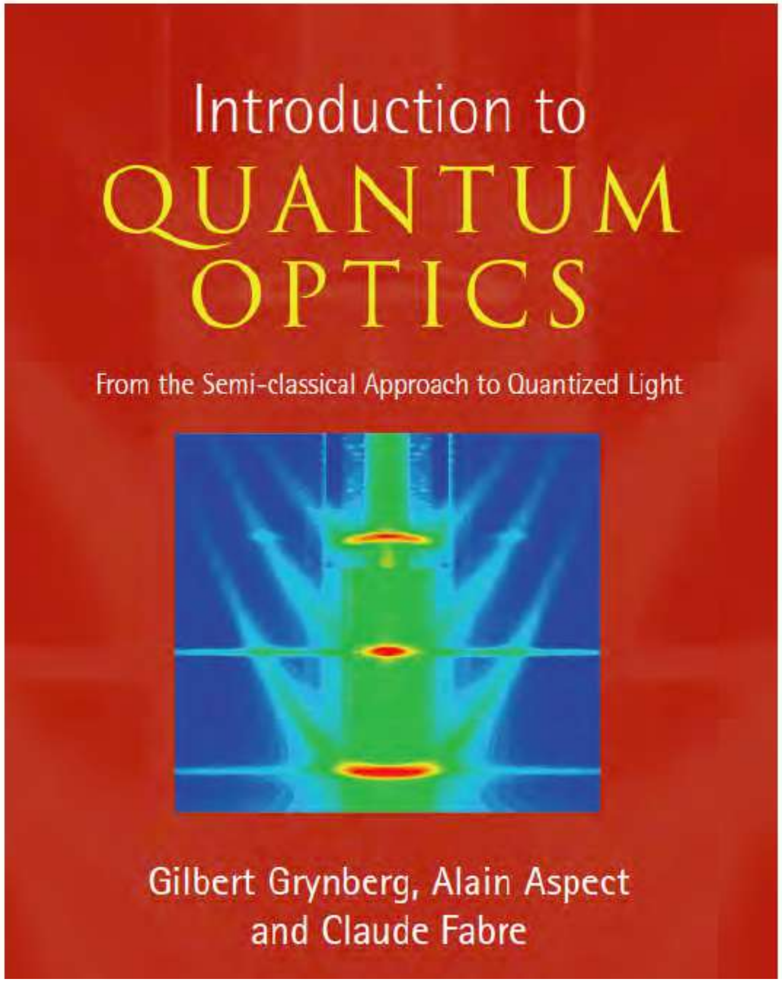

quantification requires modes

$$\hat{\mathbf{E}}^{+}(\mathbf{r},t)=\sum_{m}E_0\hat{a}_m\mathbf{f}_m(\mathbf{r},t)$$

comes from quantization procedure:
linearity of quantum mechanics

comes from electromagnetism
linearity of Maxwell equations

most general quantum state of field

$$|\Psi\rangle=\sum_{n_1=0}^{\infty}\dots\sum_{n_m=0}^{\infty}\dots C_{n_1,\dots,n_m,\dots}|n_1\,photons\,en\,\mathbf{f}_1,\dots,n_m\,photons\,en\,\mathbf{f}_m,\dots\rangle$$

double basis:
- of modes,
- of states inside each mode

both can be changed

Expérimental characterization of the temporal shape of the principal modes or "supermodes"

Experimentally Accessing the Optimal Temporal Mode of Traveling Quantum Light States

Olivier Morin, Claude Fabre, and Julien Laurat*

Laboratoire Kastler Brossel, Université Pierre et Marie Curie, Ecole Normale Supérieure, CNRS, 4 Place Jussieu, 75252 Paris Cedex 05, France

(Received 14 June 2013; published 19 November 2013)

The characterization or subsequent use of a propagating optical quantum state requires the knowledge of its precise temporal mode. Defining this mode structure very often relies on a detailed *a priori* knowledge of the used resources, when available, and can additionally call for an involved theoretical modeling. In contrast, here we report on a practical method enabling us to infer the optimal temporal mode directly from experimental data acquired via homodyne detection, without any assumptions on the state. The approach is based on a multimode analysis using eigenfunction expansion of the autocorrelation function. This capability is illustrated by experimental data from the preparation of Fock states and coherent state superposition.

DOI: 10.1103/PhysRevLett.111.213602 PACS numbers: 42.50.Dv, 03.65.Wj, 03.67.−a

conditional generation of single photons
"heralded photons"

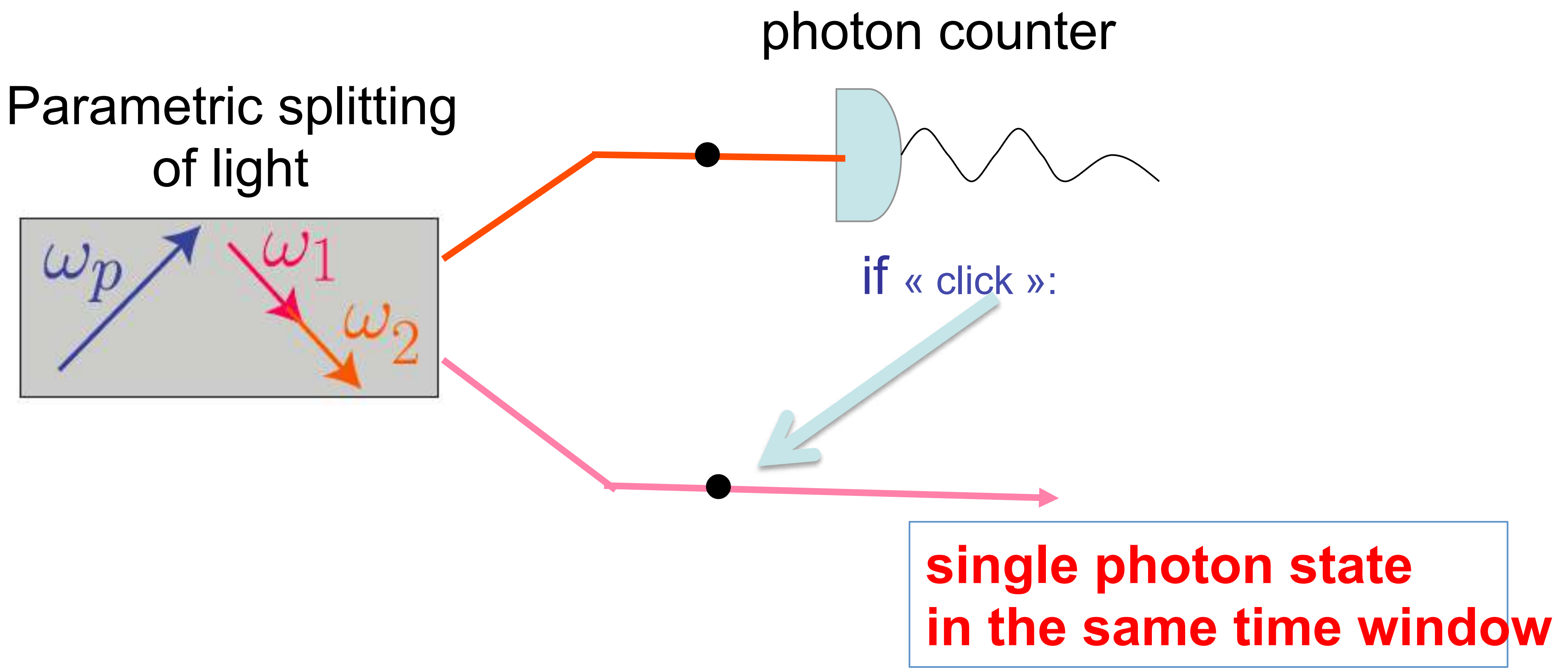

experimental set-up

Parametric crystal
inside an optical cavity

photon counter

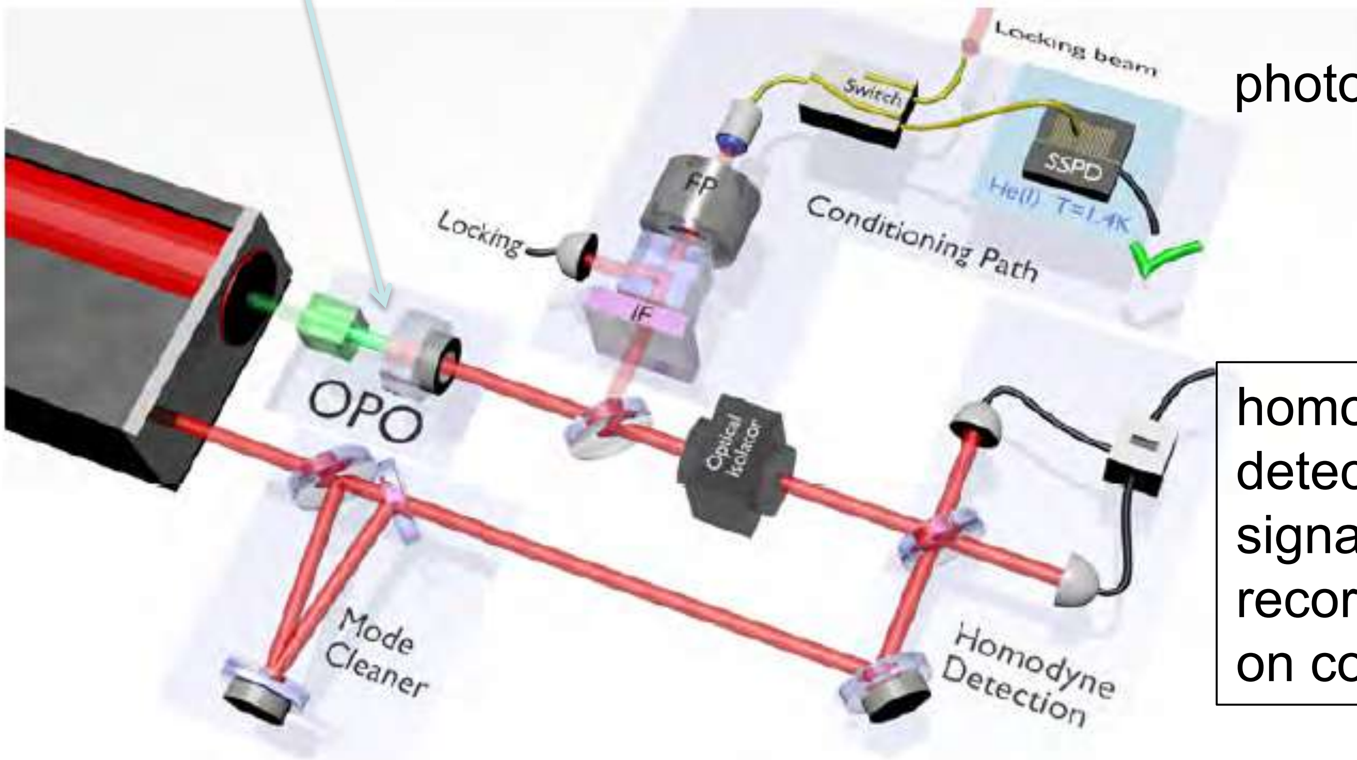

homodyne detection signal $x(t)$ recorded on computer

O. Morin et al, Phys. Rev. Letters **111**, 213602 (2013)

used modes : time bins

measured quantity :
homodyne signal
intensity during Δt

(on a given quadrature)

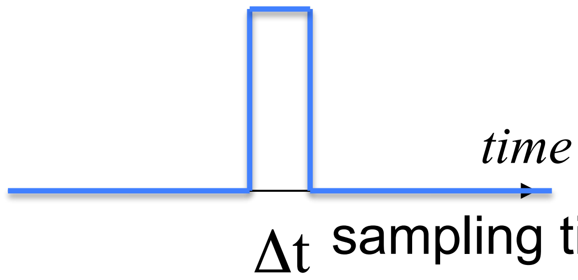

1000 measured
time bins:

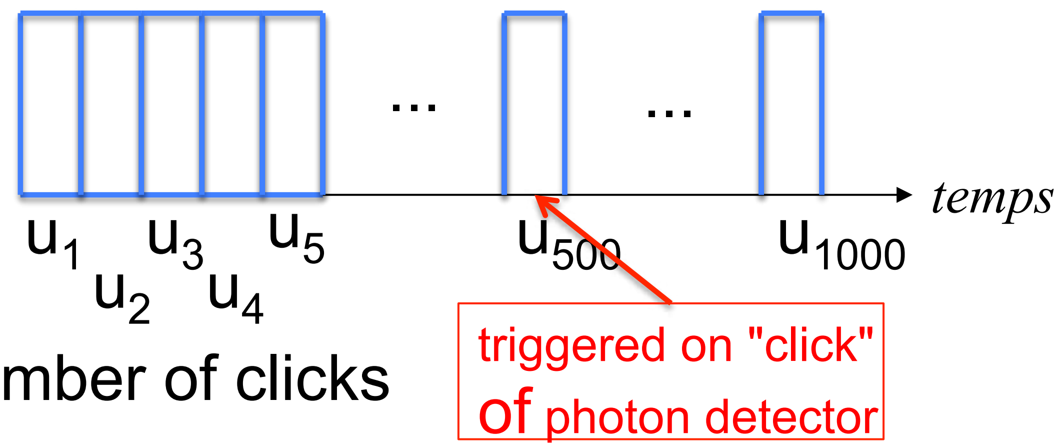

averaged over a great number of clicks

$$\begin{bmatrix} \Delta^2 E_{X1} & C(E_{X1}E_{X2}) & \dots & C(E_{X1}E_{XN}) \\ C(E_{X2}E_{X1}) & \Delta^2 E_{X2} & \dots & C(E_{X2}E_{XN}) \\ \dots & \dots & \dots & \dots \\ C(E_{XN}E_{X1}) & C(E_{XN}E_{X2}) & \dots & \Delta^2 E_{XN} \end{bmatrix}$$

1000×1000 covariance matrix of a single quadrature, which can be diagon

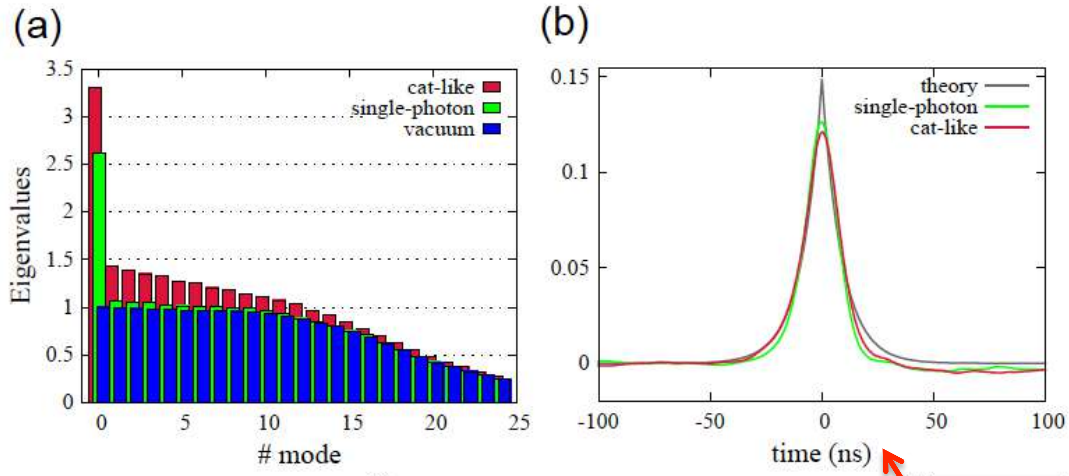

eigen values of covariance matrix

1: level of vacuum fluctuations (= E_0^2)

only one eigen value different from vacuum fluctuations

the generated state is single mode

time shape of temporal mode

it corresponds to the temporal mode of the OPO cavity
(=Fourier transform of cavity spectrum)

$$e^{-|t-t_{trigger}|/T_{cav}}$$

manipulation
of frequency modes

"quantum frequency combs"

The quantum analogue of Wavelength Division Multiplexing (WDM) ?

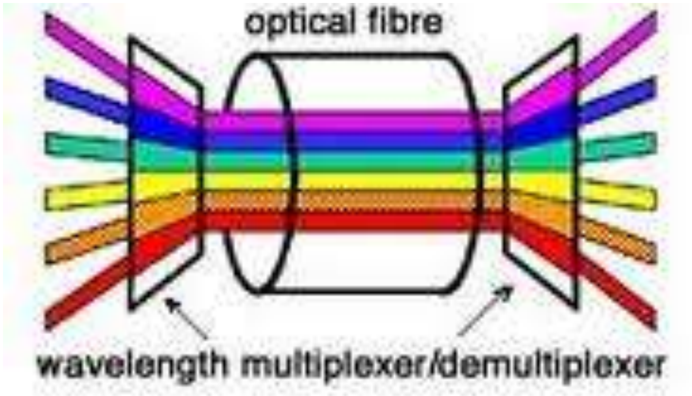

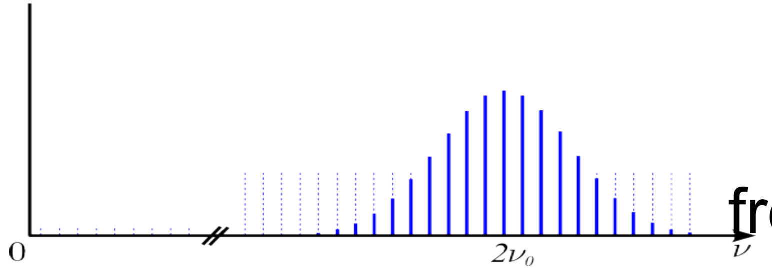

multi-frequency quantum state

many modes easily accessible :

a way to massively parallel quantum information processing ?

Balanced homodyne detection of squeezed vacuum

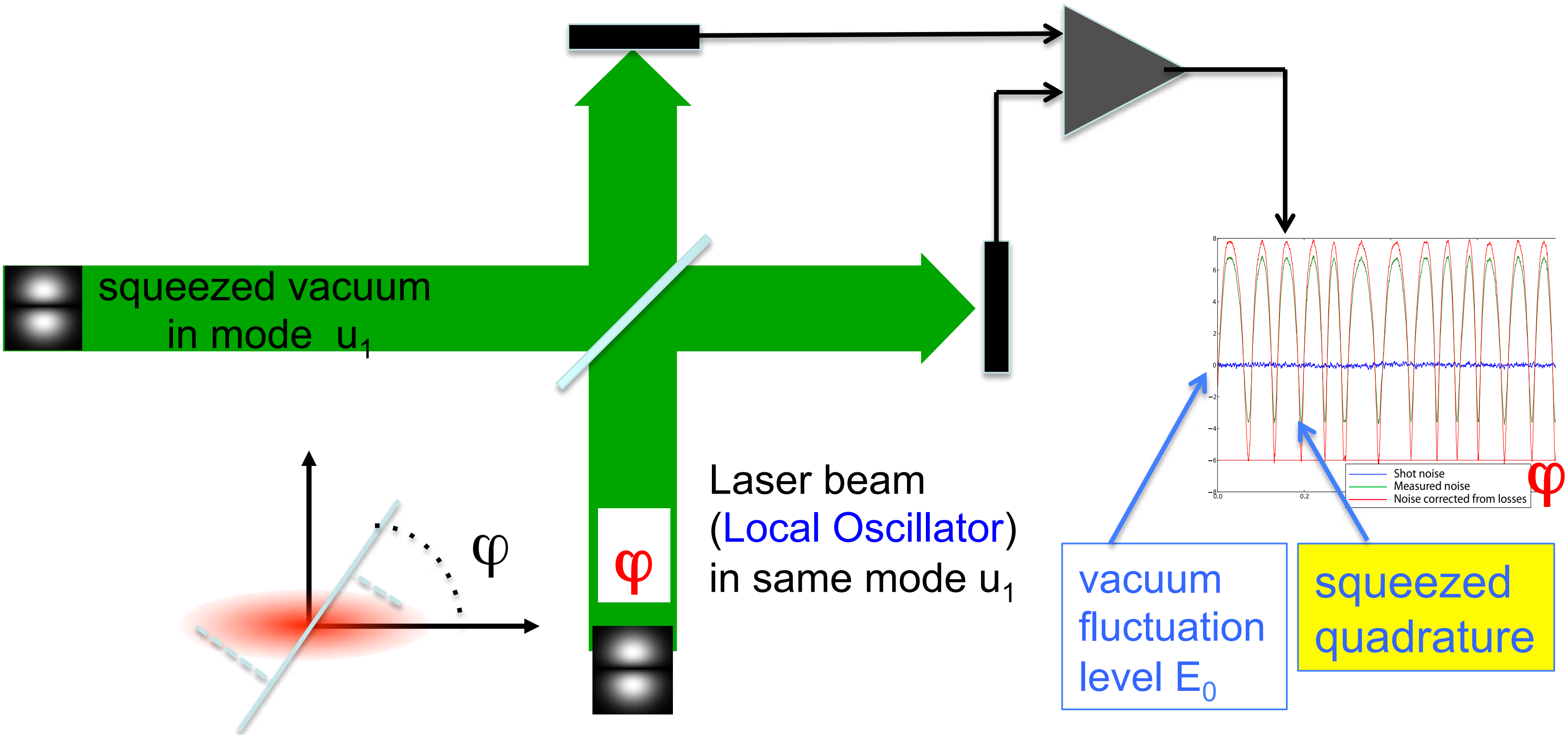

How to analyze the modal content of a multimode light state ?

- use several homodyne detections

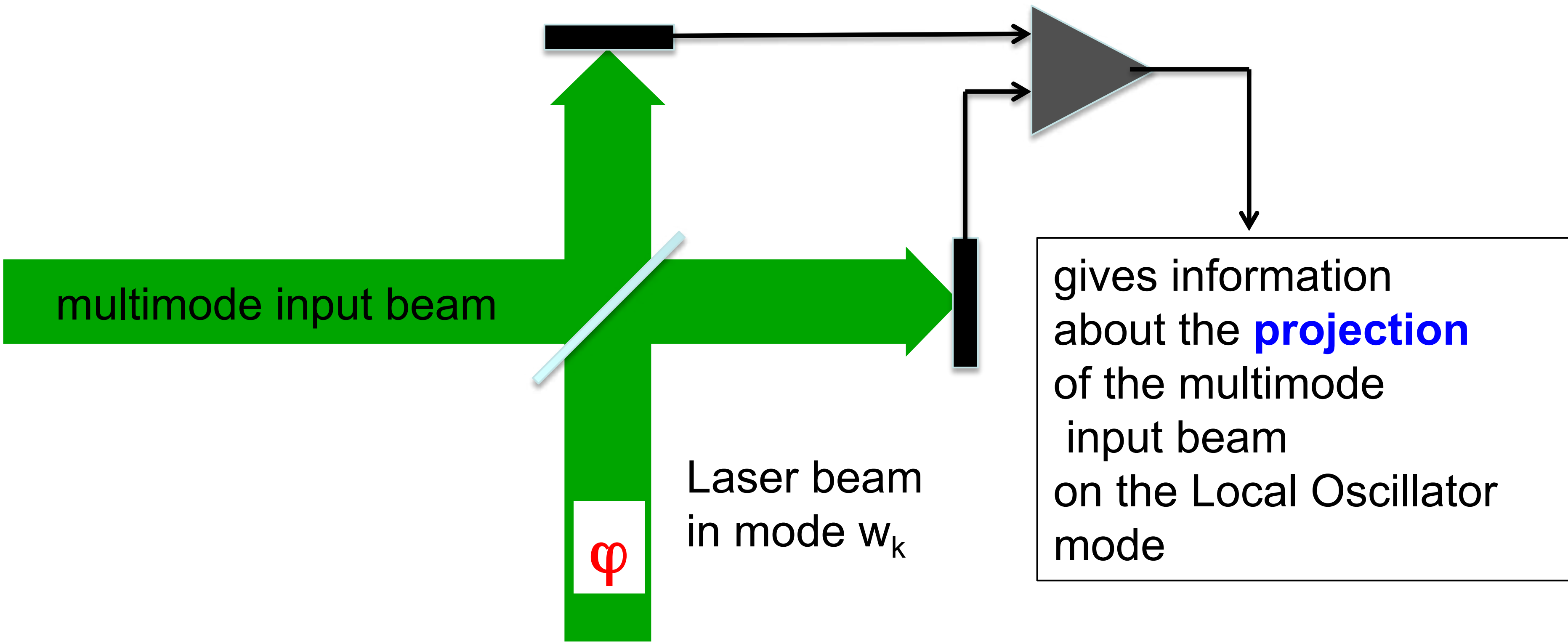

one performs a series of homodyne measurements
on a set of modes $\{\mathbf{w}_k(\mathbf{r},t)\}$

The frequency comb

optical frequency comb:

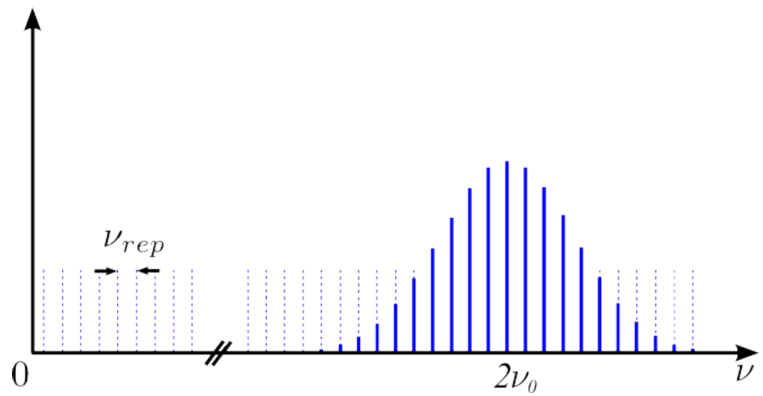

frequency

time

Frequency modes of a mode-locked laser: **about 100.000**

Can we entangle all these modes ?

Can we perform quantum computing operations on all these modes ?

Parametric down conversion of monochromatic pump

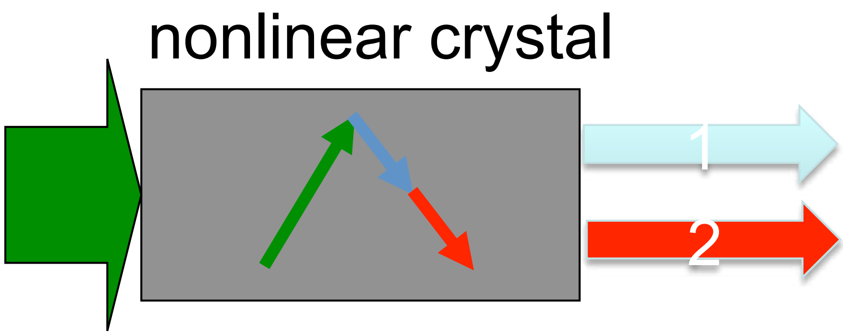

output : two mode EPR entangled state

- for a monochromatic pump

spectrum of down-converted light:

$$\nu_{signal} + \nu_{idler} = \nu_{pump}$$

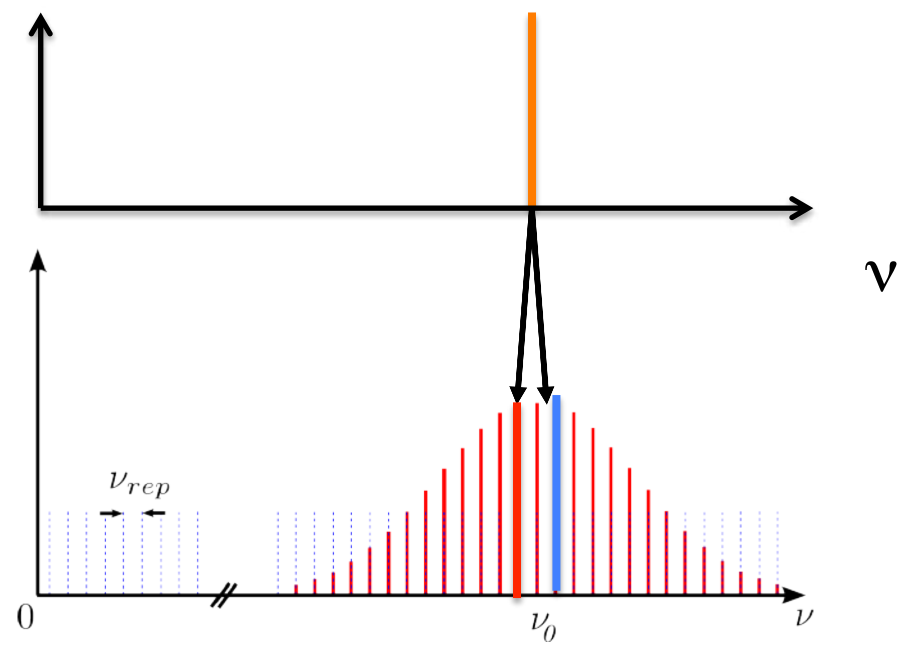

- creates independent couples of EPR entangled modes

the Synchronously Pumped Optical Parametric Oscillator (SPOPO)

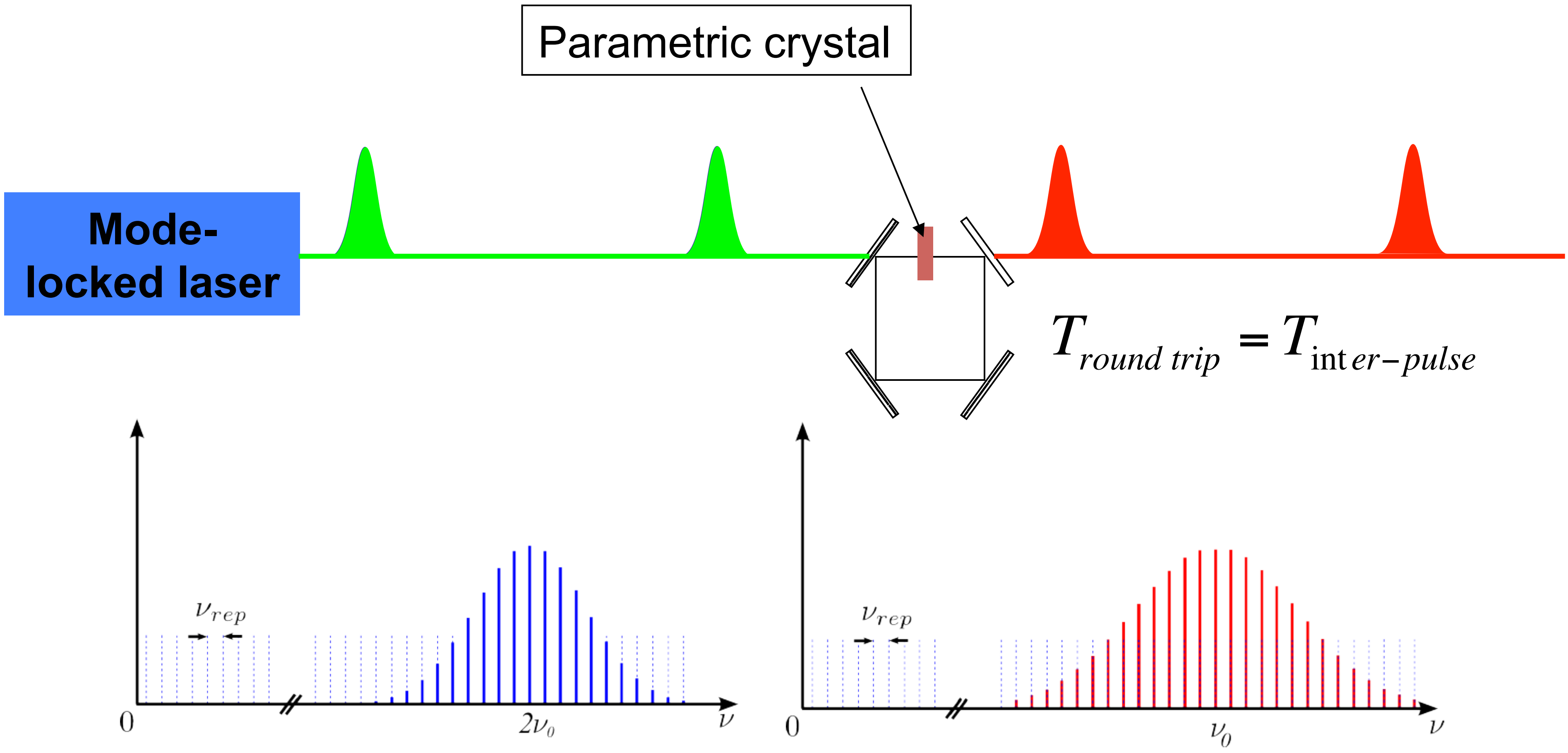

Parametric down conversion of a frequency comb

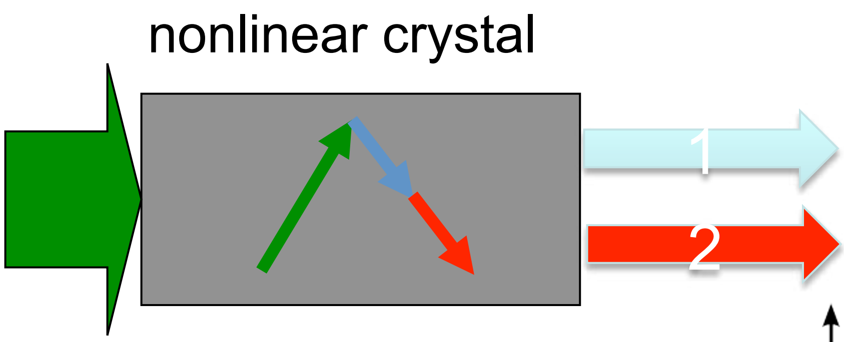

output :
two mode
EPR entangled state

- for a frequency comb pump

spectrum of down-converted light:

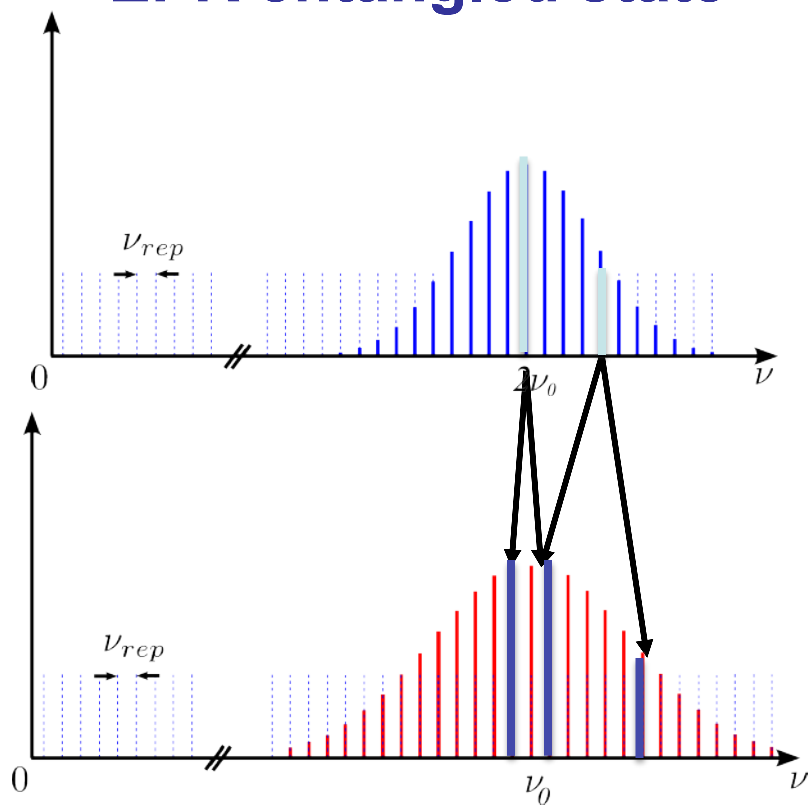

- all couples of frequencies should be entangled

A liitle bit of theory ...

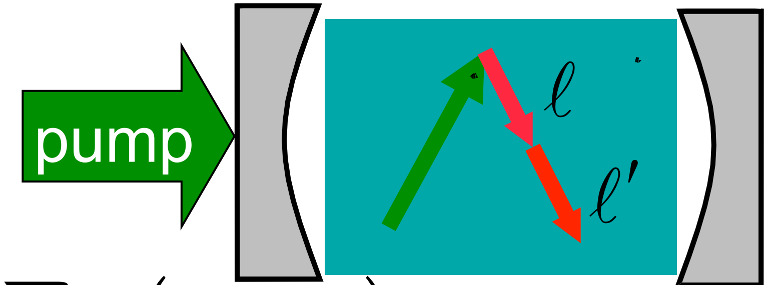

$$\hat{H} = \sum_{\ell,\ell'} \chi(\omega_\ell, \omega_{\ell'}) \; \alpha_{pump}(\omega_\ell + \omega_{\ell'}) \left(\hat{a}_\ell^+ \hat{a}_{\ell'}^+ + \hat{a}_\ell \hat{a}_{\ell'} \right)$$

Crystal phase matching coefficient

pump spectral amplitude

$$\hat{H} = \sum_{\ell,\ell'} G_{\ell,\ell'} \left(\hat{a}_\ell^+ \hat{a}_{\ell'}^+ + \hat{a}_\ell \hat{a}_{\ell'} \right)$$

Symmetrical matrix

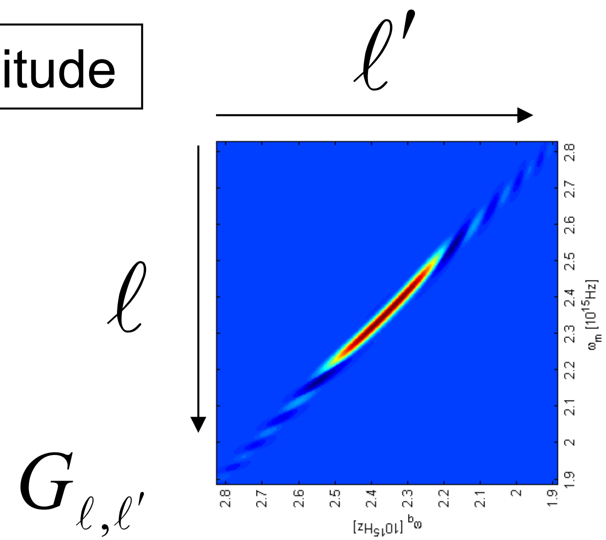

G. De Valcarcel, G. Patera, N. Treps, C. Fabre, Phys. Rev. A**74,** 061801(R) (2006)

Shifeng Jiang, N. Treps, C. Fabre, New Journal of Physics, **14** 043006 (2012)

Diagonalizing the interaction

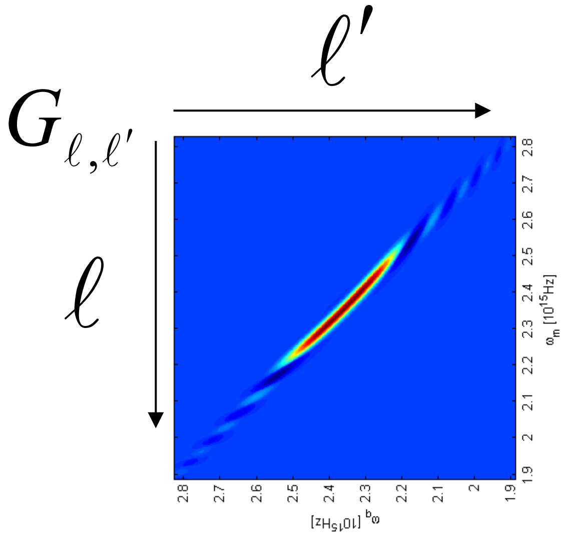

- Eigenstates:
  near combinations of frequency modes

  "supermodes" $\hat{b}_k = \sum_{\ell} U_k^{\ell} \hat{a}_{\ell}$

eigenvalues Λ_k

$$\hat{H} = \hbar \sum_{k=1}^{N_m} \Lambda_k \left(\hat{b}_k^2 + \hat{b}_k^{+2} \right)$$:multi-squeezing hamiltonian

$$\left|\Psi_{\text{out}}\right\rangle = \left|Squeezed\ state_k(\Lambda_1)\right\rangle \otimes \ldots \otimes \left|Squeezed\ state_k(\Lambda_{N_m})\right\rangle \otimes \left|0\right\rangle \otimes \ldots$$

supermode shapes

Simple example: Gaussian variation of $G_{\ell,\ell'}$

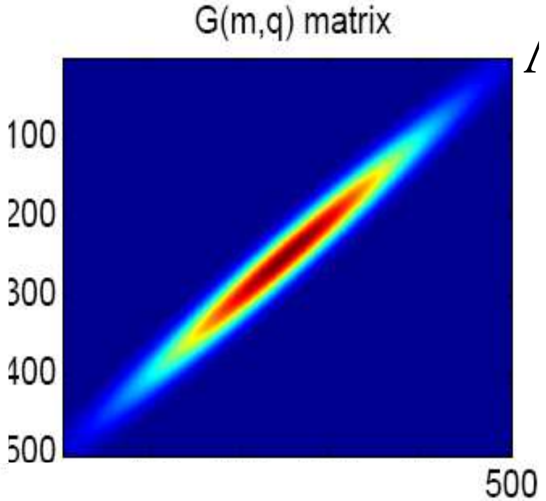

Eigenmodes: combs with Hermite-Gauss modal amplitudes

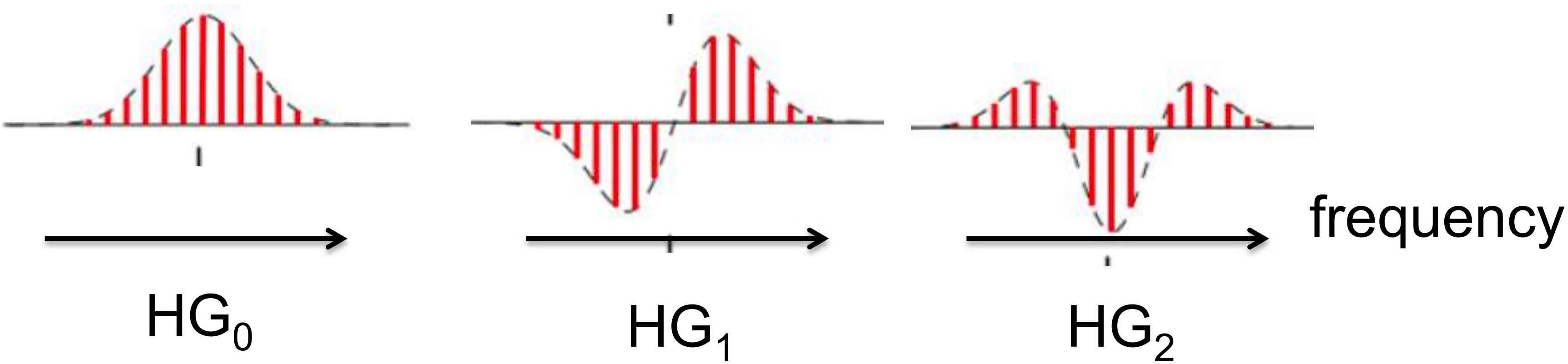

supermode shapes

Simple example: Gaussian variation of $G_{\ell,\ell'}$

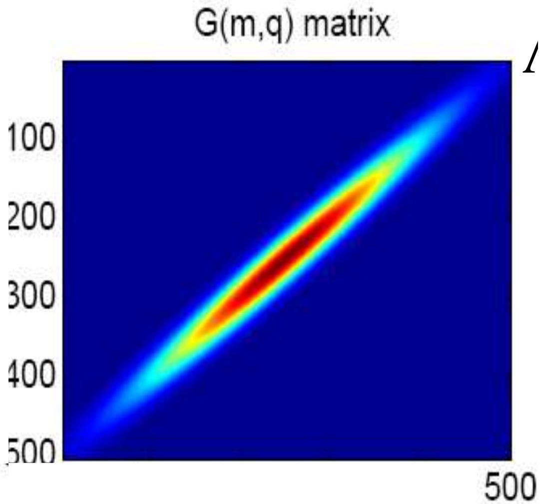

Eigenmodes: trains of pulses with Hermite-Gauss temporal shapes

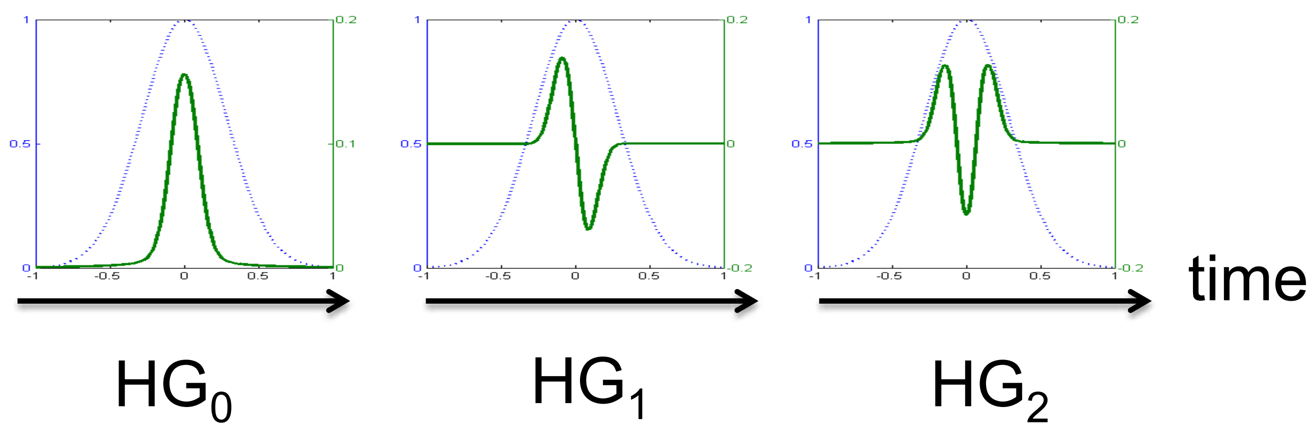

entanglement: another choice of mode basis

- Starting from two squeezed supermodes $\hat{b}_1 \quad \hat{b}_2$

the mixed modes $$\hat{b}_{\pm} = \frac{1}{\sqrt{2}}(\hat{b}_1 \pm \hat{b}_2)$$

are EPR entangled

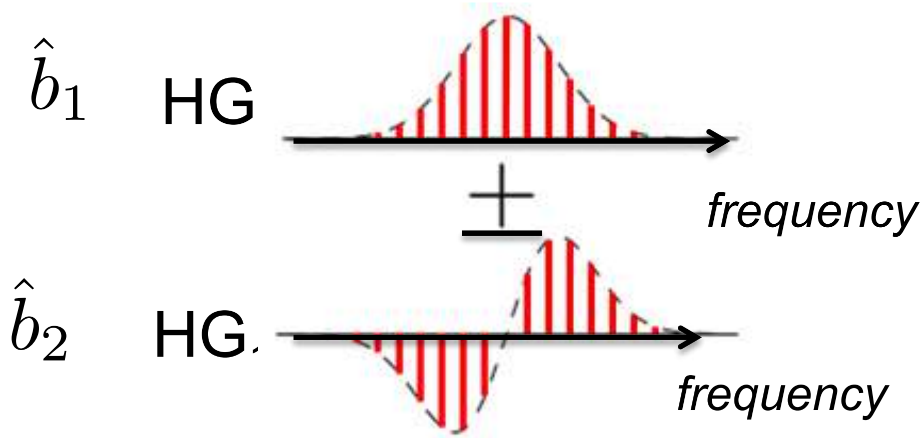

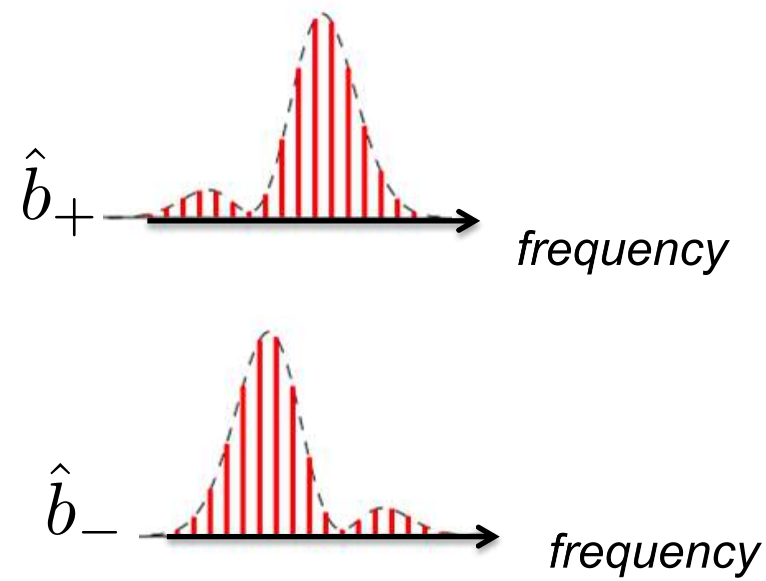

squeezed **entangled**

there will be entanglement
between different spectral parts of the comb

quantum state at SPOPO output

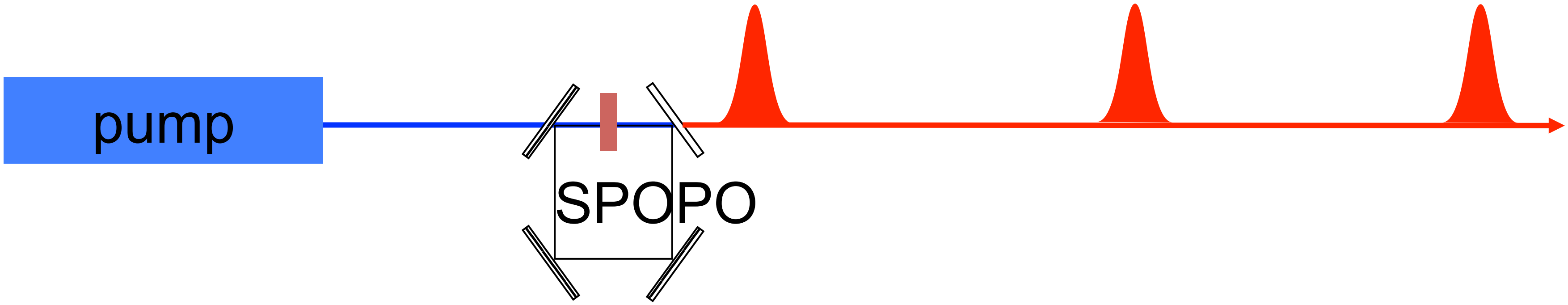

- factorized squeezed vacuum states in supermode basis

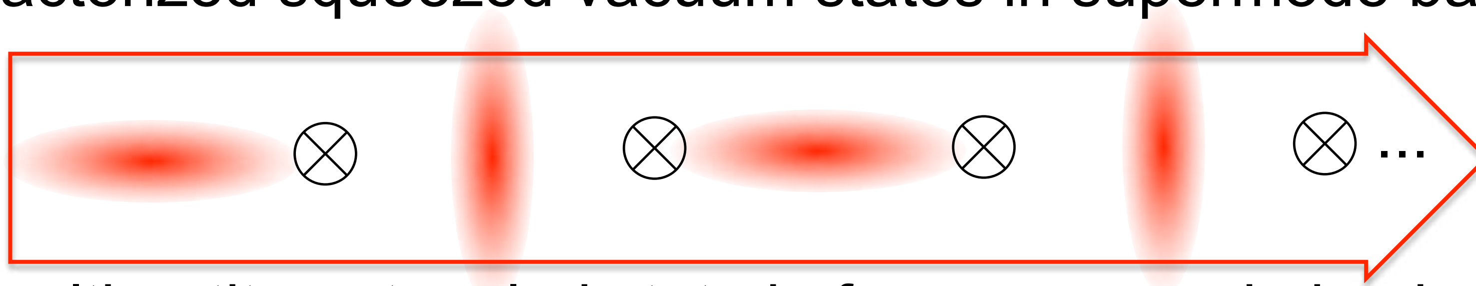

- multipartite entangled state in frequency mode basis

it depends on the way one looks at it !